

Interannual variability of summer monsoon rainfall over Myanmar

Zin Mie Mie Sein^{1,2} · Xiefei Zhi^{1,3}

Received: 10 September 2015 / Accepted: 29 April 2016 / Published online: 23 May 2016
© Saudi Society for Geosciences 2016

Abstract Observed summer (May–October) rainfall in Myanmar for the period 1981–2010 was used to investigate the interannual variability of summer monsoon rainfall over Myanmar. Empirical orthogonal function, the sequential Mann-Kendall test, power spectrum analysis, and singular value decomposition (SVD) were deployed in the study. Results from spectral analysis showed that the variability of rainfall over Myanmar exhibits a 2- to 6-year cycle. An abrupt change in rainfall over the country was noted in 1992. There was a notable increasing rainfall trend from 1989. After the sudden change, the mean rainfall increased by 36.1 mm, compared with the mean rainfall before the sudden change, and was associated with a rise in temperature of about 0.2 °C. An increase in heavy rainfall days was observed from the early 1990s to 2010. IOD and ENSO play an important role in the interannual variability of the summer rainfall over Myanmar. The covariability between rainfall over Myanmar and Indian Ocean SST generally suggests that a positive IOD mode is associated with suppressed rainfall in the central and northern

parts of Myanmar. During a negative IOD mode, nearly the whole Myanmar experiences enhanced rainfall, which is associated with devastating socioeconomic impacts. The covariability between the rainfall over Myanmar and the sea surface temperature in the Pacific Ocean in the first and second SVD modes was dominated by warming in the east and central Pacific—an El Niño-like pattern—resulting in dry conditions in central Myanmar.

Keywords Monsoon rainfall · Interannual variability · Myanmar · ENSO · IOD

Introduction

About 60 % of the world's population lives in monsoon areas. The monsoon rainfall greatly affects the agricultural yields in most developing nations (PROMISE 2003; Parthasarathy et al. 1994). Myanmar is one of the countries whose economies are mainly supported by rain-fed agriculture and related sectors. This calls for the study and understanding of rainfall variability in the country, as its occurrence can adversely affect the country's socioeconomic sector.

Myanmar is located in the northwestern part of the Indochina Peninsula (9°32'–28°31' N, 92° 10'–101° 11' E). The summer monsoon is the predominant climate system in Myanmar and nearly 90 % of total rainfalls are from the summer monsoon. Myanmar experiences five different weather seasons: pre-monsoon season from mid-April to mid-May, monsoon season from mid-May to mid-October, the post monsoon season from mid-October to end-November, the dry and cool season from end-November to mid-March, and the hot season from mid-March to mid-April (Lwin 2000; Qian and Lee 2000). This study, however, considers rainfall for the period of May to October, as the whole country is

Electronic supplementary material The online version of this article (doi:10.1007/s12517-016-2502-y) contains supplementary material, which is available to authorized users.

✉ Xiefei Zhi
zhi@nuist.edu.cn

¹ College of Atmospheric Sciences, Nanjing University of Information Science and Technology, Nanjing 210044, China

² Department of Meteorology and Hydrology, Nay Pyi Taw, Myanmar

³ Key Laboratory of Meteorological Disasters, Ministry of Education (KLME)/Joint International Research Laboratory of Climate and Environment Change (ILCEC)/Collaborative Innovation Center on Forecast and Evaluation of Meteorological Disasters (CIC-FEMD)/ Science and Technology Innovation Team for East Asian Monsoon and Regional Climate Change, Nanjing 210044, China

under the influence of the monsoon during this period, even though the monsoon onset in the southern parts of Myanmar occurs around the third week of May, and there is some rainfall in October (Sen Roy and Kaur 2000). The Bay of Bengal (BOB) (5–15° N, 90–100° E) close to Myanmar is one of the regions under the significant influence of the Asian–Pacific summer monsoon system (Wang and Lin 2002). Previous studies have pointed out that the onset of the BOB summer monsoon starts around early May (Wang and Lin 2002; Mao and Wu 2007) and withdraws in late October (Ahmed and Karmakar 1993). Wang and Lin (2002) showed that the earliest summer monsoon onset occurs over the eastern BOB around the end of April to early May in the Asian–Pacific monsoon region and also pointed out the Asian–Pacific summer monsoon schedule at various key locations, in which the southern BOB and southern Myanmar experience the earliest onset and the longest rainy season. This observation corresponds to the north–south march of the Inter-Tropical Convergence Zone.

Despite the fact that a few studies (e.g., May 2004) have projected an increase in rainfall over some parts of Myanmar, its distribution both in space and time is very important. The performance of monsoon rainfall over Myanmar depends on the dates of onset and withdrawal of the southwest monsoon (Pai and Nair 2009; Htway and Matsumoto 2011) and on intra-seasonal oscillations of dry and wet spells (Waliser et al. 2003). According to the Asia–Pacific monsoon division (Wang and Lin 2002), the country is situated between the Indian summer monsoon and a broad transitional zone of the Indochina Peninsula. The study shows that dry years have a relatively shorter monsoon duration compared with wet years. The majority of the literature dealing with Asian monsoon rainfall climatology has been devoted to depicting rainy seasons over the land and islands using rain gauge observations (Yoshino 1965; Rao 1976; Ding 1992; Chen and Yen 1994).

Most past studies of rainfall in Myanmar (Huke 1965; Maung 1945; Eguchi 1996; Moe 2002; Sen Roy and Kaur 2000; Sen Roy and Sen Roy 2011) have examined the general rainfall climatology. Sen Roy and Kaur (2000) carried out a detailed study of the summer rainfall climatology of Myanmar using 33 years (1947–1979) of station-level monthly data. The study showed the existence of five homogenous rainfall regions across the country: northern, western, central, eastern, and southern Myanmar. Their study also pointed out that the rainfall series of Myanmar shows little correspondence with neighboring Bangladesh and northeast India, even though all of them are influenced by similar weather systems. During the southwest monsoon season, the monthly mean surface air temperatures exceed 33–35 °C in the land areas of northwest India and adjoining areas (Joshi et al. 1990). The progressive development of heat lows before and during the monsoon season is considered to be one of the

major causative factors of the Indian summer monsoon circulation (Rao 1976). According to Pant and Kumar (1997), near the west coast of India, the winds are predominantly west-southwesterly to westerly, with speeds of 5–10 ms⁻¹. This pattern persists throughout the active phase of the southwest monsoon. An important part of the evolution of the monsoon circulation is the mean trough running from western Pakistan to the north of the BOB. According to Krishnamurti and Bhalme (1976), this trough extends from the sea level to 500 hPa, with a southward slope. Sen Roy and Sen Roy (2011) suggested an overall negative relationship between the El Niño Southern Oscillation (ENSO) and rainfall patterns across Myanmar, with substantial regional-level variations in the strength of the relationship. The basic dynamics of the interannual variation in the south Asian monsoon was depicted by Chen and Weng (1999b) for tropical stationary waves. Lau et al. (2000) argued that interannual variations in the south and east–southeast Asian monsoons may be dynamically independent.

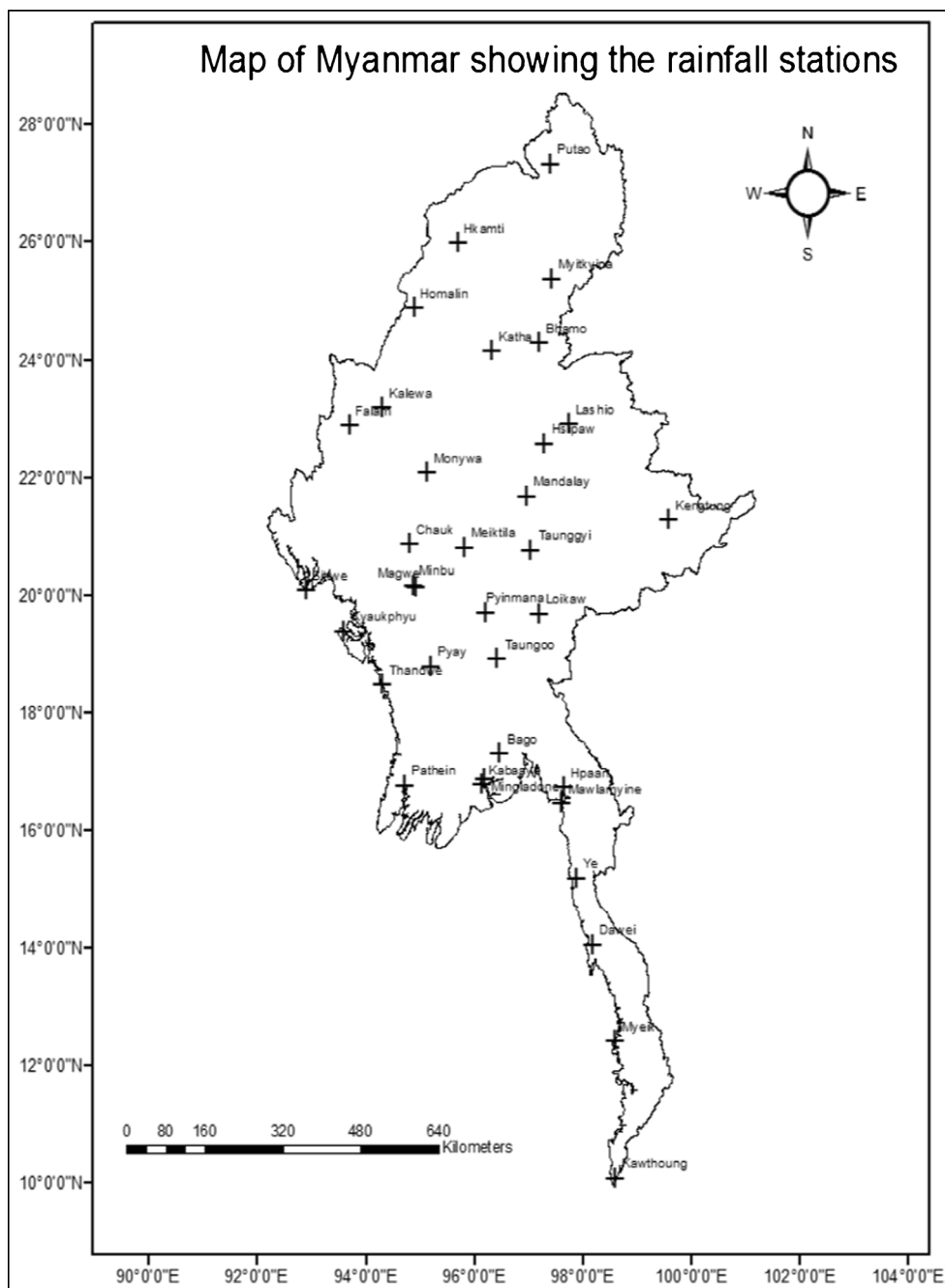
So far, no study has been carried out on the interannual variability of summer monsoon rainfall over Myanmar. The interannual variability of monsoons suggests different rainfall patterns in different places over the monsoon region. This suggests that there are other factors that need to be considered to have a clear understanding of the system. Thus, it is important to investigate the interannual variability and total areal coverage of the monsoon rainfall or seasonal rainfall (May–October) over Myanmar. In this regard, an attempt has been made to investigate the summer monsoon rainfall over Myanmar from 1981 to 2010 using composite analysis.

Data and methods

Daily rainfall data spanning from 1981 to 2010 for 35 stations in Myanmar were provided by the Department of Meteorology and Hydrology, Myanmar. The distribution of these stations is shown in Fig. 1. The meridional and zonal winds, temperature, and relative humidity data used to determine the moisture transport are the ERA-interim data, gridded at 0.75° resolution (Dee et al. 2011). The sea surface temperature (SST) data used are the Extended Reconstructed Sea Surface Temperature (ERSST) version 3b, sourced from the National Oceanic and Atmospheric Administration and National Climatic Data Center (Smith et al. 2008). The data are available on their website at <http://iridl.ldeo.columbia.edu/SOURCES/.NOAA/.NCDC/.ERSST/.version3b/.sst/>.

Empirical orthogonal function (EOF) analysis was used to investigate the dominant modes of variability of the May–October (MJJASO) rainfall over the region. The data were normalized to prevent areas (and seasons) of maximum variance from dominating the eigenvectors (Walsh and Mostek

Fig. 1 Map of Myanmar showing the rainfall stations used in the study



1980). The standardized rainfall anomaly Z was computed as expressed in Eq. 1:

$$Z = \frac{X - \bar{X}}{S_d} \tag{1}$$

where X is the observed MJJASO rainfall, \bar{X} is the long-term mean MJJASO rainfall, and S_d is the MJJASO rainfall standard deviation. The value of Z provides immediate information about the significance of a particular deviation from the mean (Kabanda and Jury 1999).

Composite analysis was used in this study. This involves identifying and averaging one or more categories of fields of a variable selected according to their association with key conditions. Results of the composites are then used to generate hypotheses for patterns that may be associated with the individual scenarios. In this study, the key conditions for the composite analysis were wet year and dry year, where the composites for wet and dry years were carried out separately, especially for wind and divergence fields. This was mainly to detect the circulation anomalies associated with wet and dry events over the region (Zhi et al. 2010; Zhang et al. 2015).

The Mann-Kendall test statistic (Mann 1945; Kendall 1975) is employed in time series analysis to detect a recognized event or change points in long-term time series. The sequential Mann-Kendall test (Sneyres 1990) is computed with ranked values y_i of the original values in the analysis $(x_1, x_2, x_3, \dots, x_n)$. The magnitudes of y_i , $(i = 1, 2, 3, \dots, n)$ are compared with y_j , $(j = 1, 2, 3, \dots, i - 1)$. For each comparison, the cases where $y_i > y_j$ are counted and denoted by n_i . A statistic t_i can therefore be defined as given in Eq. 2:

$$t_i = \sum_{j=1}^i n_i \tag{2}$$

The distribution of the test statistic t_i has a mean as expressed by Eq. 3:

$$E(t_i) = \frac{i(i-1)}{4} \tag{3}$$

and variance as in Eq. 4:

$$Var(t_i) = \frac{i(i-1)(2i+5)}{72} \tag{4}$$

The sequential values of a reduced or standardized variable, called statistic $U(F)$, are calculated for each of the test statistic variables t_i , as given in Eq. 5:

$$U(F) = \frac{[t_i - E(t_i)]}{\sqrt{Var(t_i)}} \tag{5}$$

The forward sequential statistic $U(F)$ is estimated using the original time series $(x_1, x_2, x_3, \dots, x_n)$, and the values of the backward sequential statistic $U(B)$ are estimated in the same manner but starting from the end of the series. In estimating $U(B)$, the time series is re-sorted so that the last value of the original time series comes first $(x_n, x_{n-1}, \dots, x_1)$. The sequential version of the Mann-Kendall test statistic allows detection of the approximate beginning of a developing trend. When the $U(F)$ and $U(B)$ curves are plotted, the intersection of the curves locates the approximate potential trend turning point. If the intersection of $U(F)$ and $U(B)$ occurs beyond ± 1.96 (5% level) of the standardized statistic, a detectable change at that point in the time series can be incidental. The method has been successfully used globally in trend analysis (Zhi et al. 2010; Ongoma et al. 2013; Nalley et al. 2013).

Horizontal moisture flux convergence (MFC), often referred to as moisture convergence, was displayed for wet and

dry years by vector identity. The expression for MFC is derived from the conservation of water vapor in pressure coordinates. The MFC has been discussed in detail and used by Banacos and Schultz (2005). Three climate change indices formulated by the Expert Team on Climate Change Detection and Indices (Karl et al. 1999; Caesar et al. 2006; Caesar et al. 2010) were used in this study to investigate extreme rainfall events. The indices (Table 1) are being used globally as indicators of climate variability and change (Omondi et al. 2013; Ozer and Mahamoud 2013). The indices are defined in the statistical software package RCLimDex, which was developed at the Meteorological Service of Canada.

Singular value decomposition (SVD) is a technique used in meteorological and oceanographic data analysis. The technique is applied to two equal data sets of two jointly analyzed fields to identify pairs of coupled spatiotemporal variations. In the computation, each pair explains a percentage of the covariance between the two jointly analyzed fields, allowing for extraction of dominant modes of coupled covariability between the two analyzed fields. The technique has been widely applied (Bretherton et al. 1992; Wallace et al. 1992; Tangang 1999; Juneng and Tangang 2006) because of its ease of applicability to both regularly and irregularly gridded datasets. In this work, SVD was applied to analyze the covariability between the summer monsoon rainfall over Myanmar and the sea surface temperature (SST) in the Indian and Pacific oceans.

Power spectrum analysis was employed to ascertain the multiscale temporal variations resulting from the wavelet transform employed in the long-term rainfall dataset (Gilman et al. 1963). This approach has been successfully used in several studies, including in eastern China and Korea (Kim et al. 2010) and in India (Joshi and Pandey 2011).

Results

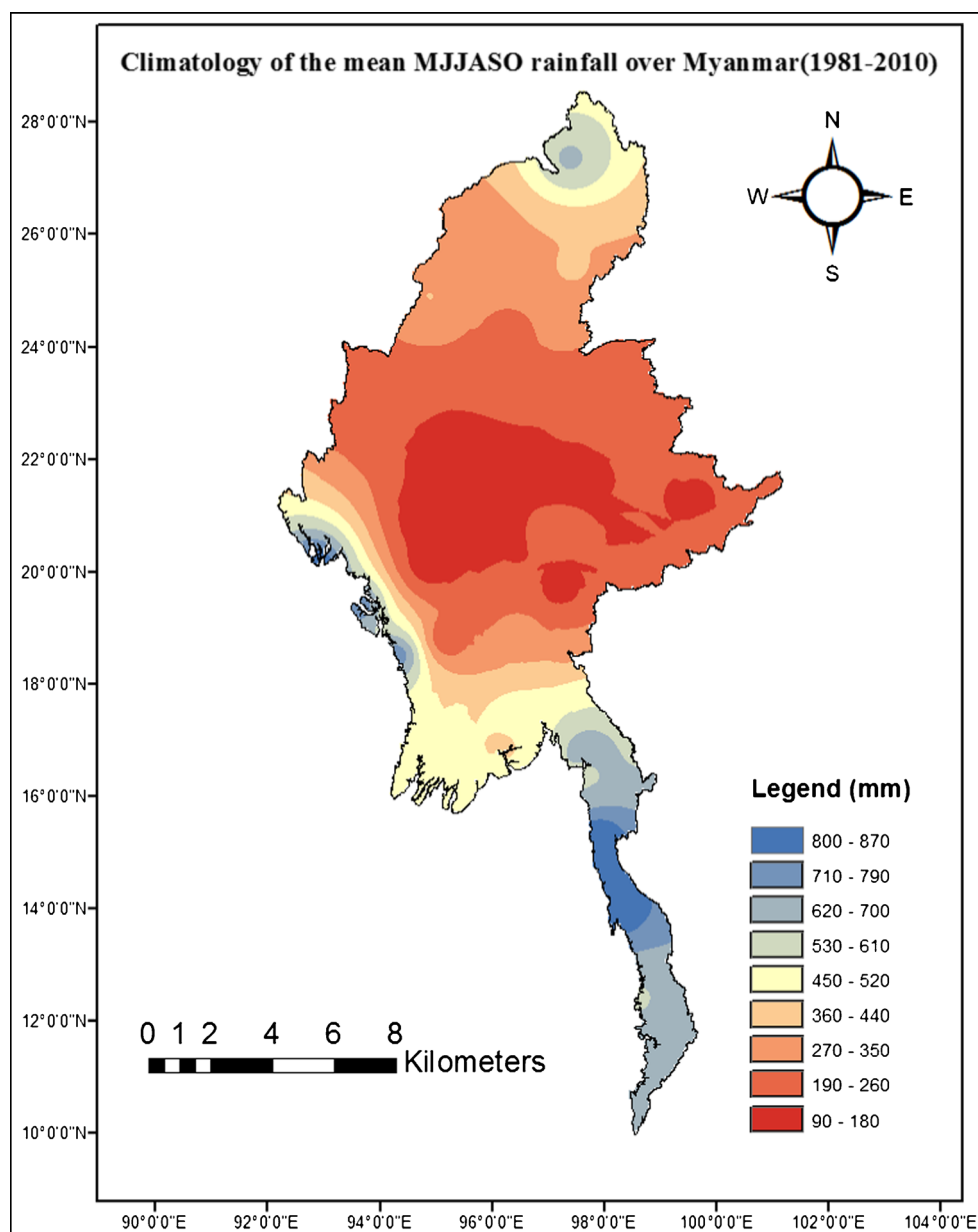
Climatology of the summer monsoon rainfall over Myanmar

The central Myanmar area (dry zone) has less rainfall compared with other areas of the country (Fig. 2). The central dry zone of the country is usually defined by three regions: Magway, Mandalay, and Sagaing. The observed low rainfall in the area can be attributed to the topography: the region is located between the north-south running mountain chains of the Rakhine-Yoma (mean elevation 1800 m, peaks 3000 m) in

Table 1 List of the expert team on climate change detection and indices climate change indices used in this study

ID	Indicator name	Description	Units
WD	Wet days	Daily precipitation ≥ 1 mm	days
R10mm	Heavy precipitation days	Annual count of days when PRCP ≥ 10 mm	days
R20mm	Very heavy precipitation days	Annual count of days when PRCP ≥ 20 mm	days

Fig. 2 Climatology of the mean MJJASO rainfall over Myanmar for the period 1981–2010

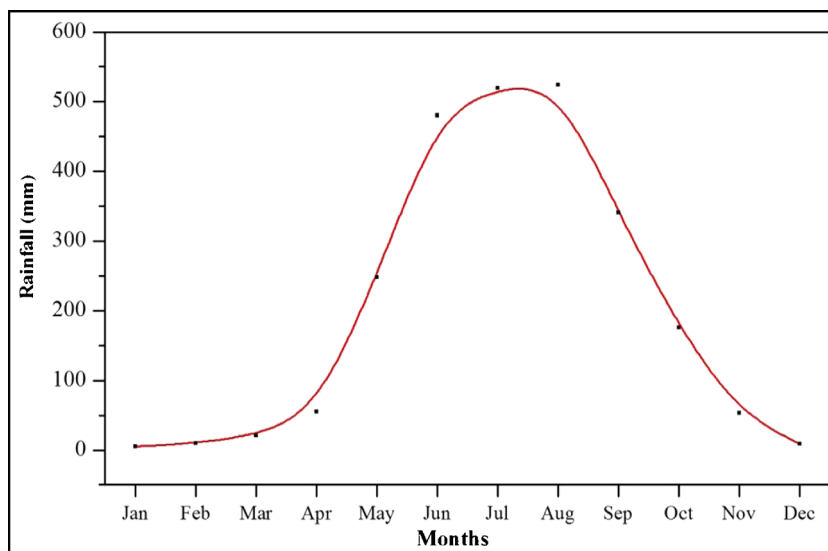


the west and Shan Plateau (mean elevation 1000–2000 m) in the east of the country. The coastal area, which is located beside the BOB and the Andaman Sea, experiences the maximum rainfall (Fig. 2). Kumar et al. (2014) and Bhowmik and Durai (2008) indicated that heavy rains along the Myanmar coast contribute more to the total rain in the Western Ghats, compared with the central and northern regions. According to studies (Kumar et al. 2014; Bhowmik and Durai 2008), the observed differences in features connecting the south and other parts of the country can be explained by linkages between cloud microphysics and large-scale dynamics.

The annual cycle of rainfall over Myanmar shows that the maximum rainfall in the region occurs in the months of June, July, and August (summer monsoon periods), as shown in Fig. 3. According to Sen Roy and Kaur (2000), the entire

country can be divided into five homogeneous rainfall zones: northern (Kachin, Sagaing above 24.5° N), western (Chin Hills, Arakan), central (Mandalay, Magwe, Sagaing below 24.5° N), eastern (Shan, Kayah), and southern (Peru, Irrawaddy, Mon, Karen, Tena_See_rim) Myanmar. In this study, the climatology of the different zones revealed that the highest rainfall region (>800 mm) lies towards the western coast and southern region (>650 mm), due to the closeness of the BOB and Andaman Sea (Fig. 4). The lowest amount of rainfall received was in the central region (dry zones), where <100 mm of rainfall is received during the monsoon (Fig 2). Sen Roy and Kaur (2000) showed that the central plains have relatively flat gradients, and this spatial distribution is caused by orographic effects, the behavior of the monsoon low and the Tibetan anticyclone.

Fig. 3 The mean annual cycle of rainfall over Myanmar for the period 1981–2010



Interannual variations of rainfall and associated circulations

The MJJASO rainfall showed an increasing trend over the region (Fig. 5). The increasing trend in rainfall is exhibited by the positive slope of the interannual rainfall variability. In addition, there were four typical wet years (1994, 1997, 2001, and 2007) and three typical dry years (1983, 1987, and 1998) during 1981–2010. These years were chosen based on standardized rainfall anomaly ≤ -1 (for dry years) and $\geq +1$ (for wet years), as used globally, e.g., Tan et al. (2014) in China, Joseph (2014) in India, and Ogwang et al. (2015) in East Africa. These years were then considered as composite years in further analysis to reveal the circulation anomalies associated with the noted extreme rainfall events.

Analysis of wind anomalies revealed that during wet years, there was an anomalous cyclonic circulation (low-pressure area) over central Myanmar, as opposed to the dry years,

which exhibited an anomalous anticyclonic circulation (high-pressure area) over central Myanmar at low level (Fig. 6).

Further examination of the pressure vertical velocity (ω) showed that wet years are associated with rising air motion (Fig. 7a). The rising motion is associated with low-level convergence and upper-level divergence. During dry years, sinking motion, low-level divergence, and upper-level convergence are shown over Myanmar (Fig. 7b). Barry and Chorley (2003) observed that convergence at low level leads to vertical stretching, whereas divergence at low level results in vertical shrinking, which suppresses convection due to subsidence. Ogwang et al. (2015) reported similar patterns while studying seasonal rainfall over East Africa. Moreover, analysis of the mean moisture transport (Fig. 8a) showed that wet years are dominated by anomalous moisture convergence (positive anomalies) at low level (850 hPa), particularly over central Myanmar. During dry years, anomalous moisture

Fig. 4 Different regions of mean summer rainfall (May–October) over Myanmar during 1981–2010

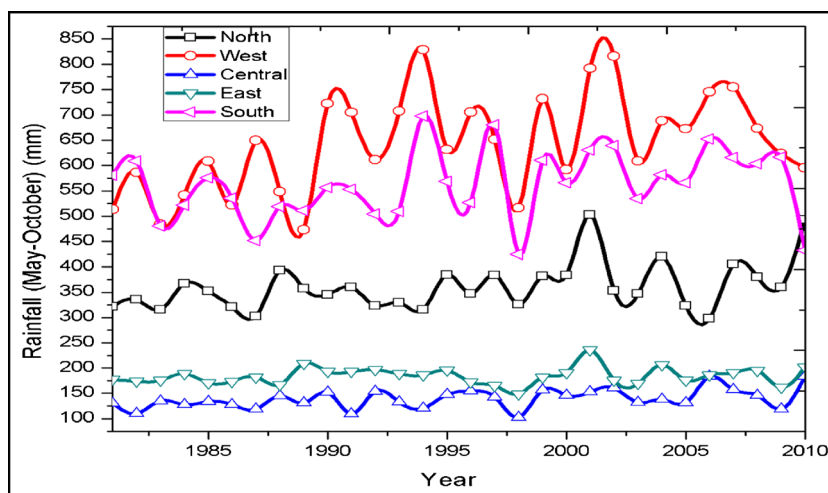
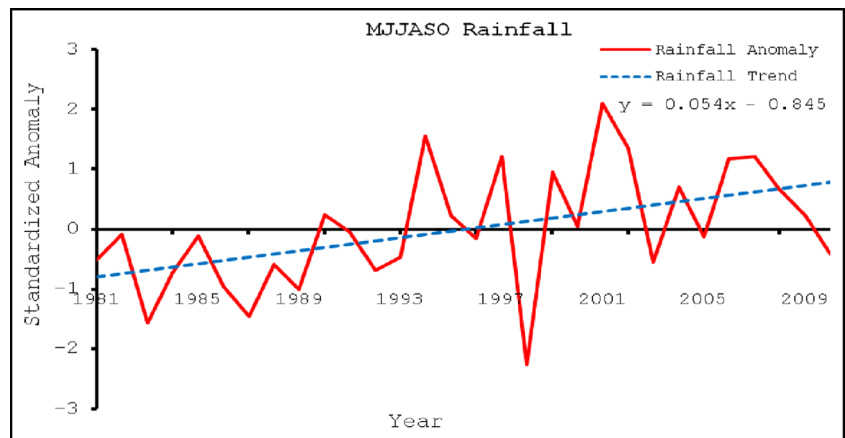


Fig. 5 The interannual variability of the mean MJJASO rainfall over Myanmar. The rainfall trend is indicated by the *dashed line*



divergence (negative anomalies) is exhibited in the same region (Fig. 8b). Li and Zhou (2016) found that the moisture circulation response to the variation of the India-Burma Trough shows great baroclinicity over the BOB.

Separate investigation of the role of wind and moisture disturbances showed that the abnormal moisture flux is dominated by the wind disturbance, as is the abnormal moisture divergence in the lower level; while that in the upper level is dominated by both wind and moisture disturbances. Further analysis of the long-term mean moisture transport at the 850 hPa level during 1981 to 2010 is shown in Fig. 9. The results show that the majority of moisture was transported to Myanmar by southwesterly and westerly winds. The strongest transport was in the southern region and on the west coast near the BOB and the Andaman Sea, and the weakest transport was in the northern and central areas. Zhang et al. (2015) employed composite analysis to examine the associated circulation anomalies of anomalous rainfall in southeast China on interannual time scales. They reported that warm and humid air from the Indian Ocean is transported to South China, and moisture transport over South China Sea (SCS) is strengthened. Two major transport channels are observed: one extends from the North Indian Ocean through India and the BOB to

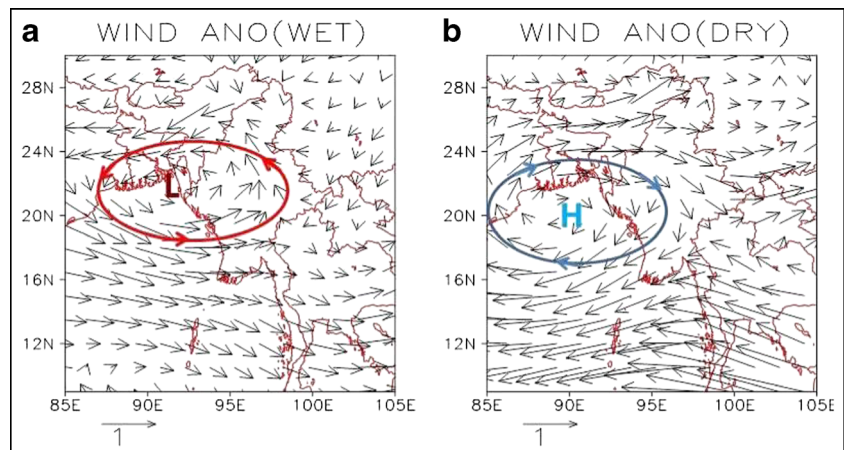
southwest China, and the other from the South Pacific Ocean through the maritime continents and the SCS towards South China. These two anomalous moisture flux channels transport warm moist air northward from the tropical oceans and thus contribute to positive specific humidity anomalies in the coastal areas of southeast China, where warm air from the south combined with cold air from the north provide favorable conditions for rainfall formation.

Detection of abrupt change in frequency and intensity of summer monsoon rainfall

Results from the Mann-Kendall test showed that there was a general decrease in the mean MJJASO rainfall between 1981 and 1989 (Fig. 10). Thereafter, the rainfall maintained an increasing trend, with a sudden change in climate in 1992. After the change, there was a notable increasing trend, which briefly became significant in 1997. After 2000, the increasing trend continued significantly until the end of the study period (2010).

Further analysis of rainfall before and after the observed abrupt change in climate revealed that the mean rainfall after the sudden change of climate (1993–2010) increased by

Fig. 6 The mean MJJASO wind anomaly over Myanmar during wet years (a) and dry years (b) where L denotes region of anomalous low pressure and cyclonic circulation, and H denotes region of anomalous high pressure and anticyclonic circulation



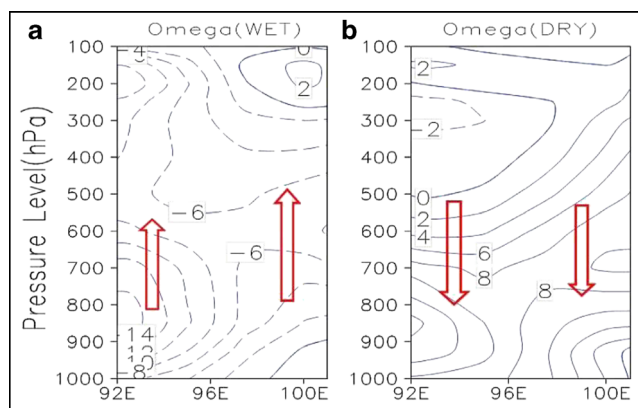


Fig. 7 The mean MJJASO omega (ω) anomaly ($\times 10^{-3} \text{ Pa s}^{-1}$) over Myanmar at latitude 20° N during wet years (a) and dry years (b) The upward arrow signifies anomalous rising motion and low level convergence and downward arrow signifies anomalous sinking motion and low level divergence

36.1 mm, compared with the mean rainfall before (1981–1991) the observed change in 1992 (Table 2). Further investigation showed that the increased change in rainfall may be associated with the rise in temperature in the region, which was noted to have increased by 0.2° C after the sudden change, compared with the mean value before the observed change. Zhi et al. (2010) indicated that the winter climate in southern China experienced a sudden change around 1991, and the surface air temperature and extreme rainfall increased significantly after 1991 compared with those before the sudden change. Our present study found similar phenomena in different seasons and different regions. This may further be linked to climate change, which is the main focus of this study.

Results from the analysis of climate change indices show that the number of heavy rainfall days ($\geq 10 \text{ mm}$) (Fig. 11) and very heavy rainfall days ($\geq 20 \text{ mm}$) (Fig. 12) generally increased throughout the study period, and the change was

significant at the 95 % confidence level. The change may similarly be attributed to the observed global warming. The abrupt change in trend in both cases is observed to occur in the early 1990s. The increase in extreme events is a possible indicator of climate change in Myanmar and its surrounding areas. The heavy rainfall events are associated with flash floods across Myanmar, which cause loss of lives and destruction of property.

Spatial and temporal distribution and patterns of summer rainfall

The spatial component of the first eigenvectors (EOF1) of the mean MJJASO seasonal rainfall more or less exhibited a dipole mode (pattern) of variability, explaining 24 % of the total variance, with strong positive loadings in the western coast and southern sector of the region, and strong negative loadings in the northern and central sectors (Fig. 13a). The results agreed with other studies. Zveryaev and Aleksandrova (2004) found the first EOF mode explains 24.17 % of the total variance of JJAS rainfall over Southeast Asia, and its spatial pattern is characterized by rainfall variations, with the strongest signal being near the BOB (the western coast and southern sector of Myanmar). The west coast and southern region showed strong positive loadings due to them receiving the strongest moisture from the Indian Ocean (Fig. 9), which also agreed with the observation of the highest rainfall over those two regions (Fig. 4). The northern and central sector loadings were strongly negative according to the weakened moisture transport (Fig. 9) and corresponded to the least amount of rainfall received in the central (arid zones) and northern regions (Fig. 4). The principal component (PC) time series corresponding to EOF1 (PC1) is shown in Fig. 13b. The second EOF (EOF2) explaining 16 % of the total variance showed a

Fig. 8 The mean MJJASO moisture transport (MTR) at 850 hPa in $\text{g kg}^{-1} \text{ ms}^{-1}$ over Myanmar during wet years (a) and dry years (b) based on ERA interim dataset. Vectors show moisture transport, whereas the shaded regions indicate convergence (positive) and divergence (negative) of moisture fluxes. The circled areas in yellow show convergence and divergence zones in Fig. 8a and 8b, respectively

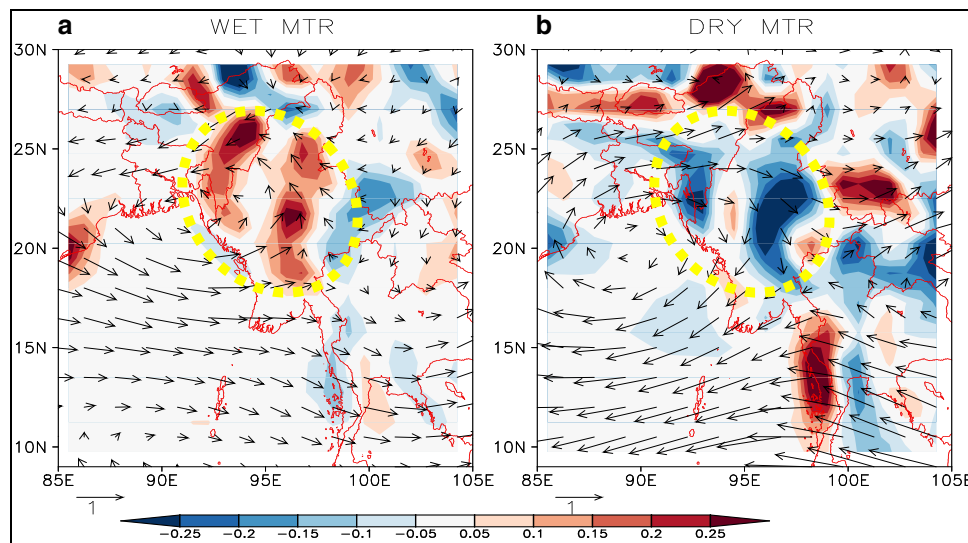
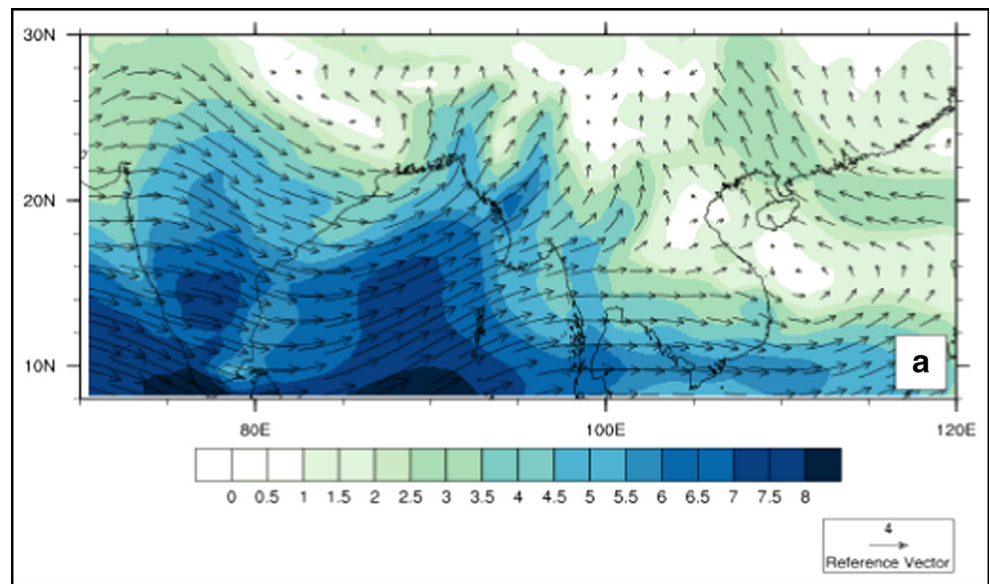


Fig. 9 Long-term mean MJJASO moisture transport (MTR) at 850 hPa ($\text{g kg}^{-1} \text{ms}^{-1}$) over Myanmar during the period 1981–2010 based on the ERA interim dataset. Vectors show moisture transport and the shading indicates the moisture



dipole pattern, with the opposite pattern to EOF1 (Fig. 13c). This observation is also in agreement with Sein et al. (2015). The PC time series related to EOF2 (PC2) is shown in Fig. 13d. The result of EOF3 explains 9 % of the total variance, with positive loadings in northern region and negative loadings in the central region and southern tip of Myanmar (Fig. 13e). The time series of the corresponding PC connected to EOF3 (PC3) is shown in Fig. 13f. Ge et al. (2016) found that the interannual variability of summer monsoon rainfall (1979–2011) over the Indochina Peninsula is characterized by EOF1 of 5-month total rainfall (May to September). The leading mode, with a monopole pattern, accounts for 30.6 % of the total variance. The rainy season rainfall over the Indochina Peninsula is linked to ENSO on interannual scales. The interannual variation of tropical cyclones modulated by ENSO is a significant contributing factor to the rainy season rainfall over the Indochina Peninsula.

To verify the significance of the scales of interannual variation, the power spectra of the summer rainfall in Myanmar for a period of 30 years were analyzed. The power spectra in Myanmar showed significant spectral peaks, at approximately 5 to 6 years, which is also at an interannual timescale (Fig. 14). The power spectra show that in central Myanmar a significant spectral peak occurs at approximately 3 to 6 years and in northern Myanmar at 3.5 years, while western Myanmar shows a significant spectral peak at approximately 2 to 3 years, as shown in Fig. 14. Some scientists also indicated that there is a significant period of 2 to 3 years in the precipitation over East China where the East Asian monsoon dominates (Zhu and Zhi 1991; Zhi 1997; Yang et al. 2011 among others). It is worth noting that no significant spectral peak is observed in the southern and eastern Myanmar areas at the 90 % confidence level. This happens despite the fact that the southern region generally receives higher rainfall compared

Fig. 10 Mann-Kendall analysis of summer monsoon rainfall (MJJASO) during 1981–2010 over Myanmar. The dashed lines, above and below the line denoting zero represent significant at 95 % confidence level

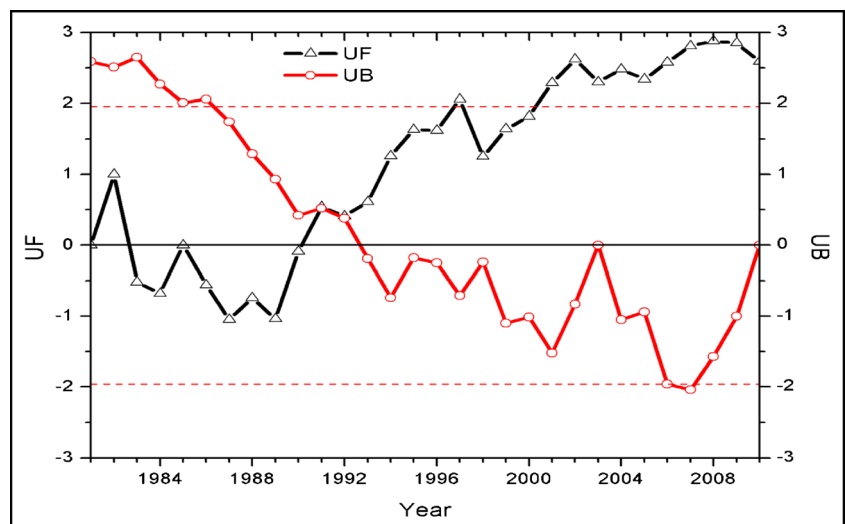


Table 2 Mean May–October rainfall (RF) and temperature (TMP), showing the long-term mean (LTM, 1981–2010), the mean values before the change in 1992, and the mean values after the change (1993–2010). Rainfall difference (RFD) and temperature difference (TMPD) denote rainfall and temperature difference between the mean values (after change minus before change), before and after the observed change in 1992

	RF (mm)	TMP (°C)	RFD (mm)	TMPD (°C)
LTM (1981–2010)	485.1	22.8		
Before change (1981–1991)	463.6	22.7		
After change (1993–2010)	499.7	22.9	36.1	0.2

with the other regions, with the exception of the western region. This suggests possible difficulty in long-term rainfall forecasting over the eastern and southern regions.

Relationship between SST in the Indian and Pacific oceans and rainfall over Myanmar

To examine the link between rainfall over Myanmar, and Indian Ocean and Pacific Ocean SST, SVD analysis was carried out to understand the covariance matrices of the two fields. The findings are shown using heterogeneous correlation patterns, as demonstrated by Wallace et al. (1992). A statistical summary for the first three SVD modes of Indian Ocean SST and Myanmar rainfall, including the percentage of squared covariance explained by each mode, the temporal correlation between pairs of expansion coefficients, and the variance in individual fields that are explained by each mode, is presented in Table 3. In summation, the three modes account for 84 % of the squared covariance between the two fields and the corresponding components explain 61 % (43 %) of the SST (rainfall) variance. The first SVD mode explains 43 % of the squared covariance between Indian

Ocean SST and rainfall, and its heterogeneous correlation patterns are shown in Fig. 15a,b. The SST pattern itself explains 34 % of the total SST variance (Table 3). This mode is characterized by a positive Indian Ocean Dipole (IOD): anomalous cooling (warming) to the east (west) of Indian Ocean (Fig. 15a). As a result of these changes, the normal convection situated over the eastern Indian Ocean warm pool shifts to the west and results in drought over the Myanmar region, especially in central area and northern areas, as observed in Fig. 15b. The first rainfall mode explains 11 % of the total rainfall variance over Myanmar and has a well-defined pattern over the domain. The second SVD mode explains 28 % of the squared covariance between Indian Ocean SST and rainfall. The SST pattern of the second SVD mode (Fig. 15c) shows the opposite pattern of SST to SVD mode 1. The SST pattern in SVD2 is explained by a negative IOD mode, associated with enhanced rainfall over central and northern Myanmar. The second rainfall mode explains 20 % of the rainfall variance, almost twice that of mode 1, thus indicating a strong association between Myanmar summer rainfall and a negative IOD. In the second rainfall mode, the variance shows much rainfall in the central region and low rainfall in the western coast and southern areas (Fig. 15d). The third SVD mode explains 13 % of the squared covariance between SST and rainfall. The Indian Ocean SST in the third SVD equally shows a negative IOD, almost similar to the observations in SVD2. The third rainfall mode accounts for 12 % of the rainfall variance, with a similar rainfall pattern to that observed in the second rainfall mode (Fig. 15f). The IOD in the third SVD is, however, weak, evidenced by the weak east–west SST differences, resulting in less rainfall compared with rainfall in mode 2. This affirms the effect of the IOD on rainfall over Myanmar. Figure 16 gives a time series of the expansion coefficients for the three SVD modes of Indian Ocean SST and Myanmar rainfall. The temporal correlation between the SST in the central and eastern Indian Ocean and rainfall time series

Fig. 11 Mann-Kendall analysis of heavy precipitation (≥ 10 mm per day) during MJJASO 1981–2010 over Myanmar. The dashed lines, above and below the line denoting zero represent significant at 95 % confidence level

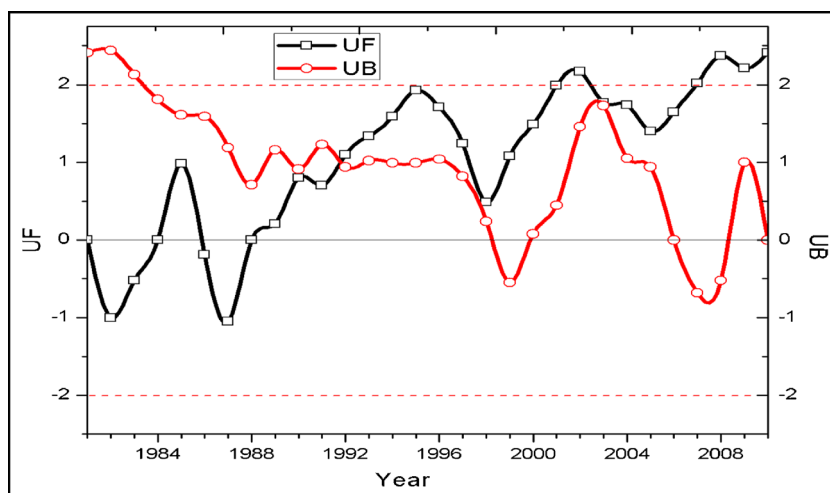
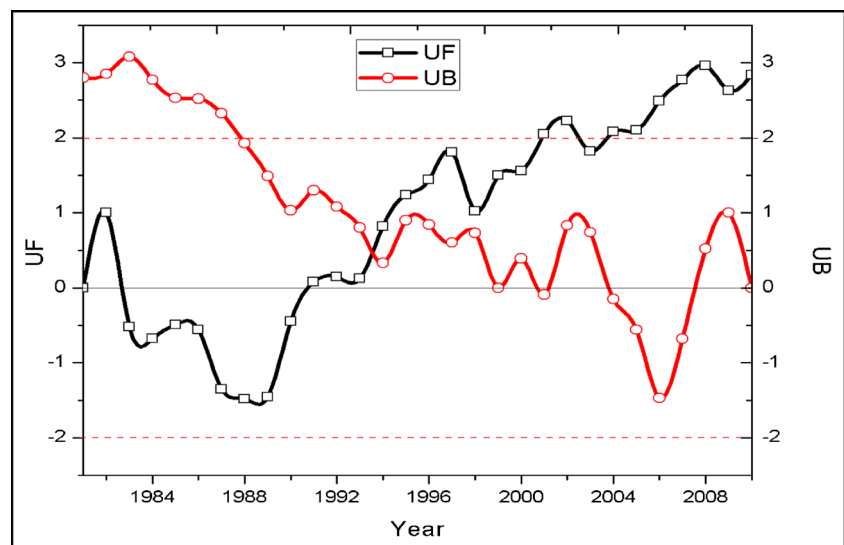


Fig. 12 Mann-Kendall analysis of very heavy precipitation (≥ 20 mm per day) during MJJASO1981–2010 over Myanmar. The dashed lines, above and below the line denoting zero represent significant at 95 % confidence level



in mode 1 is 0.69—the highest among the three modes (Fig. 16a). The correlation between the pairs of mode 2 (3) is 0.64 (0.61) (Fig. 16b,c).

The statistics for the first three SVD modes of Pacific Ocean SST and Myanmar rainfall, including the percentage of squared covariance explained by each mode, the temporal correlation between pairs of expansion coefficients, and the variance in individual fields that are explained by each mode are given in Table 4. In total, the three modes account for 87 % of the squared covariance between the two fields, and the corresponding components explain 60 % of the SST variance and 42 % of the rainfall variance, respectively. Modes 1, 2, and 3 of covariability of Myanmar rainfall and Pacific Ocean SST are presented in Fig. 17. The SVD mode 1 of covariability of Pacific Ocean SST and Myanmar rainfall explains 48 % of the squared covariance between the two variables. Its heterogeneous correlation patterns are shown in Fig. 17a, b. The SST pattern itself explains 33 % of the total SST variance (Table 4). This mode is characterized by the El Niño SST pattern—increasing positive correlation from the central to eastern equatorial Pacific (Fig. 17a). The first rainfall mode explains 16 % of the total Myanmar rainfall variance. The rainfall mode shows low rainfall in central and northern parts of the country, while the southern region shows high rainfall (Fig. 17b). Thus, the El Niño SST pattern is associated with drought conditions in the central and northern parts of the country, while the southern region experiences enhanced rainfall. The second SVD mode explains 31 % of the squared covariance between SST and rainfall (Table 4). This second SST mode displays large positive correlations with the central Pacific, termed the central Pacific El Niño pattern (Fig. 17c). The second rainfall mode explains 20 % of the rainfall variance, slightly higher than the first mode. The rainfall variance results show a similar pattern to the mode 1 rainfall pattern—low (high) rainfall in the central (western coast and southern) region, as shown in Fig. 17d. This is an affirmation that an

El Niño event is associated with dry conditions in the central and northern regions and normal to slightly enhanced rainfall in the western coast and southern regions of the country. The third SVD mode explains 8 % of the squared covariance between SST and rainfall. The third SST mode exhibits a negative correlation in most parts of the equatorial Pacific Ocean, as shown in Fig 17e. The third mode accounts for 6 % of rainfall variance, with generally most parts of the country receiving high rainfall, except for the south tip of country (Fig. 17f). The time series of the expansion coefficients for the three SVD modes of Pacific Ocean SST and Myanmar rainfall are presented in Fig. 18. The temporal correlation between the western Pacific Ocean SST and rainfall time series in mode 1 is 0.74. The correlations between the pairs of mode 2 and 3 are 0.80 and 0.79, respectively (Fig. 18b,c). In other studies, e.g., Dube et al. (1990), it has been reported that the interannual variability of the upper-layer thickness of the central Arabian Sea has a good correlation with Indian summer monsoon rainfall (ISMR). Ali et al. (2015) reported that the entire BOB has no significant correlation between ISMR and ocean mean temperature from January to May, indicating that the Arabian Sea may play a more prominent role in the variability of ISMR than the BOB. Joseph et al. (2013) found that ISMR exhibits prominent interannual variability, and a season of deficient June to September monsoon rainfall in India is followed by SST anomalies over the tropical Indian Ocean and cold SST anomalies over the western Pacific Ocean. Ge et al. (2016) indicated that the rainy season rainfall over the Indochina Peninsula is linked to ENSO on interannual scales based on dynamic composites and linear regression analysis. During a La Niña year, more westward-propagating tropical cyclones are generated in the northwest quadrant of the western North Pacific. These tropical cyclones develop vigorously and provide heavy rainfall over the Indochina Peninsula.

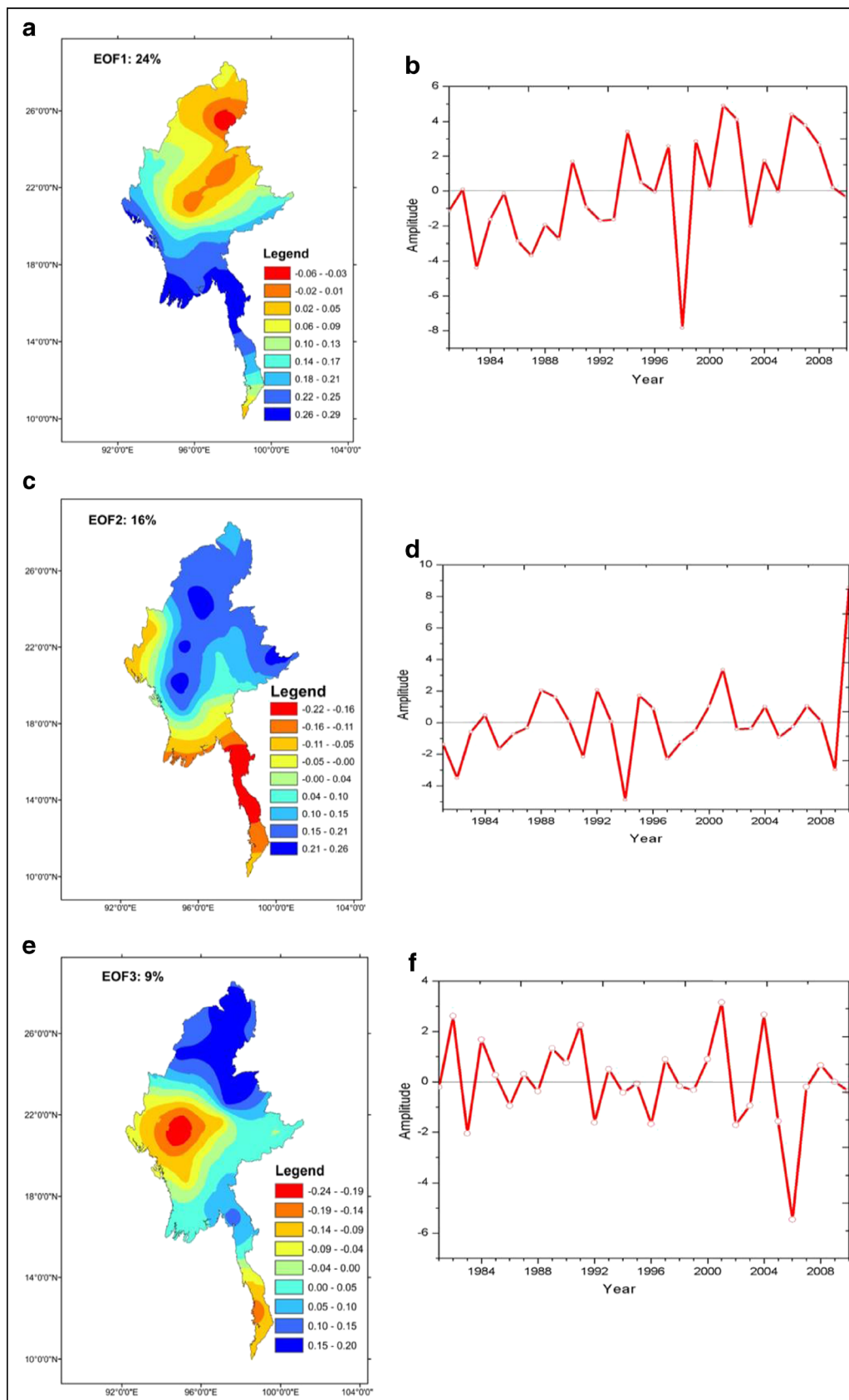


Fig. 13 The first EOF (EOF1) spatial mode of the mean MJJASO rainfall over Myanmar (a) and its time series (b); the second EOF (EOF2) spatial mode (c) and its time series (d); the third EOF (EOF3) spatial mode (e) and its time series (f)

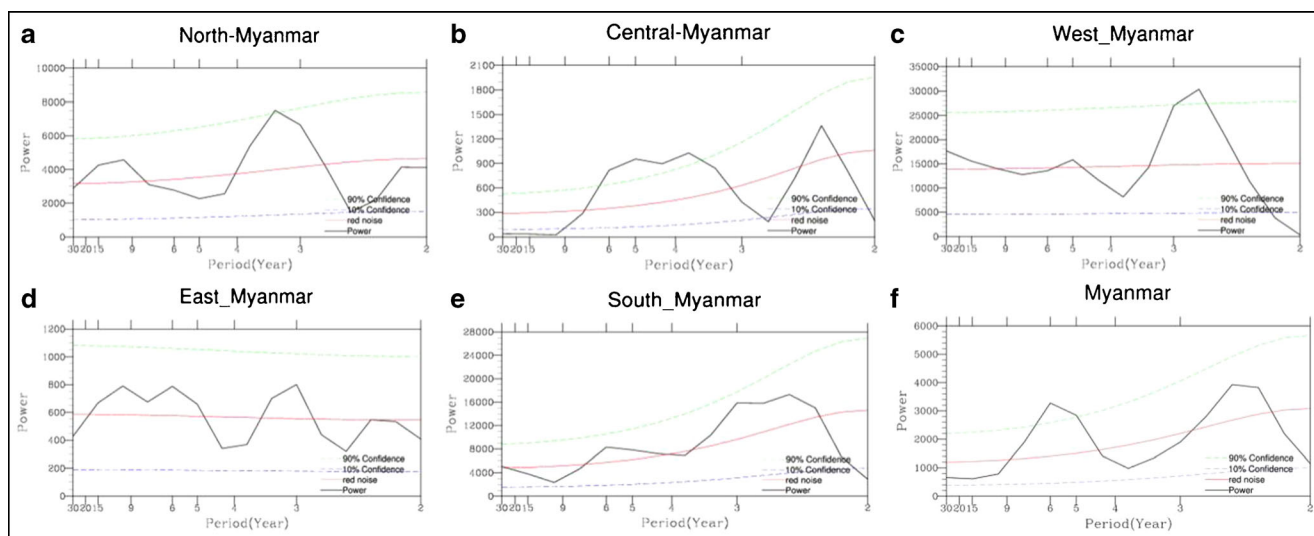


Fig. 14 Power spectra of the rainfall over north Myanmar (a), central Myanmar (b), west Myanmar (c), east Myanmar (d), south Myanmar (e), and the whole region (f). The red line indicates the Markov “red noise”

spectrum and the green dashed line denotes the 90 % significance and the blue dashed line denotes the 10 % significance boundary for the Markove Analysis

Conclusions

This study examined the summer monsoon rainfall of Myanmar for the period 1981–2010 and yielded some interesting results. The years 1994, 1997, 2001, and 2007 were noted to be extreme wet years, while 1983, 1987, and 1998 were extreme dry years. The spatial and temporal distribution and patterns of summer rainfall were significant. The dominant mode of the summer rainfall variability exhibited a dipole pattern, with dryness in the northern and central parts of Myanmar and wetness in the western and southern parts of the country, which explains 24 % of the total variance. The spectral analysis showed that the variability of rainfall over Myanmar exhibits a 2–6-year cycle, while western Myanmar shows a significant spectral peak at approximately 2–3 years.

There was a general decrease in the mean MJJASO rainfall between 1981 and 1989. Thereafter, the rainfall maintained an increasing trend, with a sudden change in rainfall in 1992. After the change, there was a notable increasing trend, which was briefly significant in 1997. After 2000, the increasing trend continued significantly until the end of the study period (2010). Further analysis of rainfall before and after the observed abrupt change in climate revealed that the mean rainfall

after the abrupt change of climate (1993–2010) increased by 36.1 mm, compared with the mean rainfall before (1981–1991) the observed change in 1992. Further investigation showed that the change (increase) in rainfall may be associated with the rise in temperature in the region, which was noted to have increased by 0.2 °C after the abrupt change, compared with the mean value before the observed change. This may further be linked to climate change, which is currently a global challenge. The study revealed an increase in heavy rainfall days, starting from the early 1990s. This calls for appropriate adaptation measures to possible flash floods that are associated with heavy rainfall over Myanmar.

The first SVD mode of Indian Ocean SST captures the Myanmar rainfall variability linked to a positive IOD mode, which is associated with low rainfall in the central and northern regions and high rainfall in the southern region. The second and third SVD mode of Indian Ocean SST revealed that a negative IOD mode generally gives low rainfall in the south, increasing northwards—the opposite pattern of the observation in the first mode. The covariability between rainfall over Myanmar and Indian Ocean SST generally shows that a positive IOD mode is associated with suppressed rainfall in the central and northern parts of Myanmar. During a negative IOD mode, nearly the whole of Myanmar experiences enhanced

Table 3 Statistics of the leading SVD Indian Ocean SST and rainfall modes

	Squared covariance	Temporal correlation	SST variance	Rainfall variance
Mode 1	43 %	0.69	34 %	11 %
Mode 2	28 %	0.64	14 %	20 %
Mode 3	13 %	0.61	13 %	12 %

SVD: Indian SST vs. Myanmar rainfall

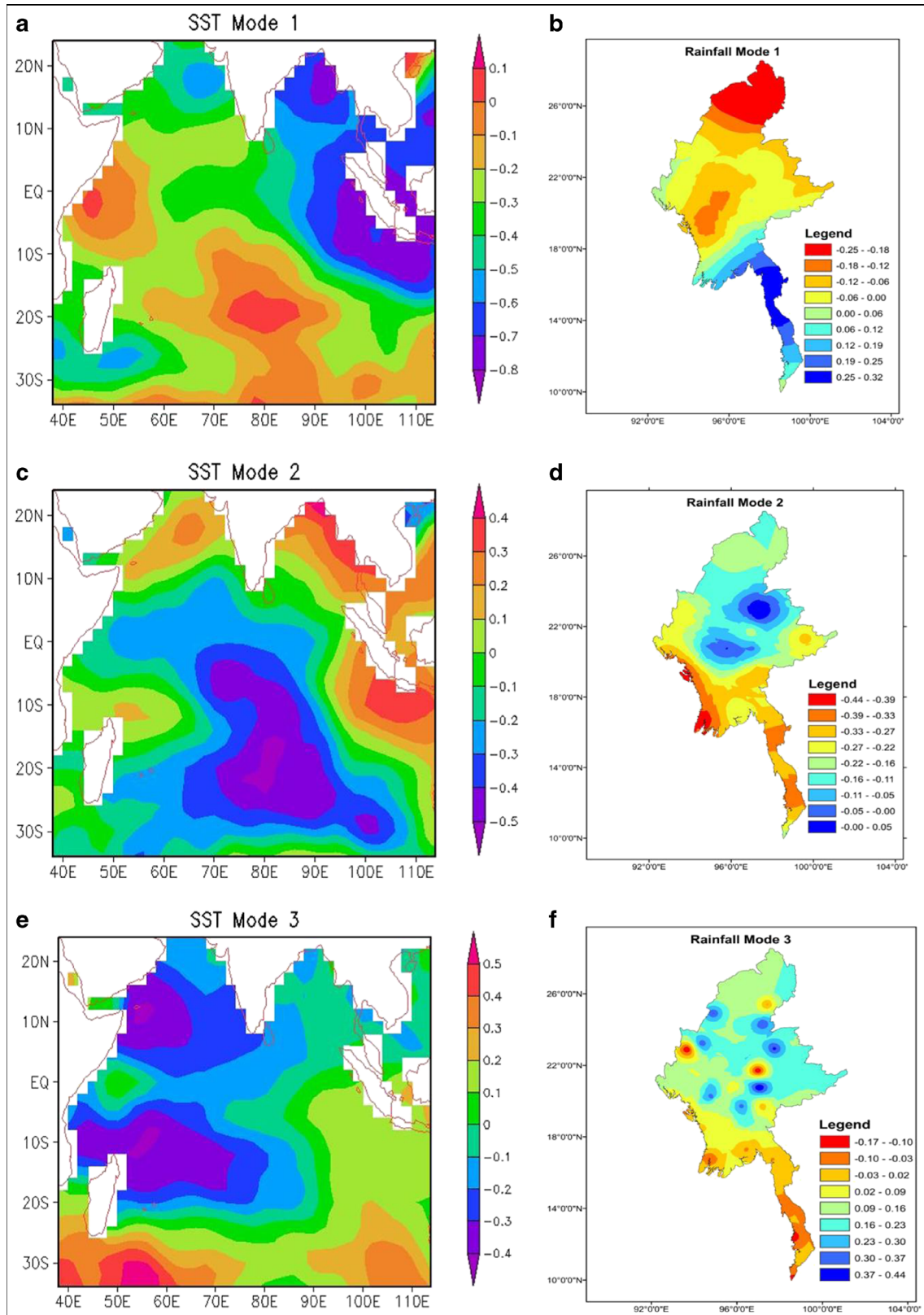
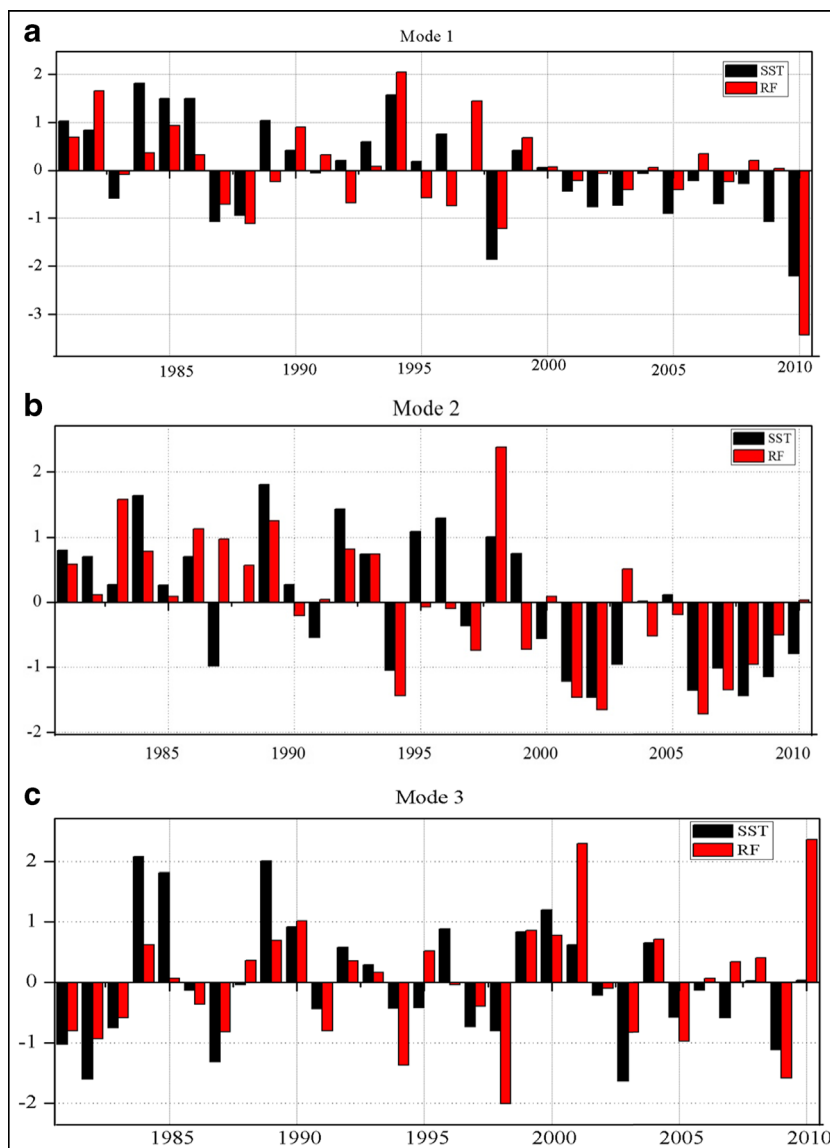


Fig. 15 Heterogeneous correlations of the first three SVD modes between Indian SST (35° S–25° N) and Myanmar rainfall

Fig. 16 Normalized time series of the first three SVD modes for Indian SST (*black bar*) and Myanmar Rainfall (*red bar*)



rainfall, which is associated with devastating socioeconomic impacts.

The covariability between the rainfall over Myanmar and the SST in Pacific Ocean in SVD modes 1 and 2 are dominated by an El Niño pattern: warming in the east and central Pacific Ocean. Rainfall modes 1 and 2 show low rainfall in the central and northern parts of the country, and high rainfall in the western coast and southern

Myanmar. Thus, an El Niño event is linked to dry conditions in the central and northern regions. Drought conditions have devastating effects on the economy of the region and the country at large, as the country’s economy is mainly reliant on rain-fed sectors. The third SST mode exhibits cooling in the most parts of the equatorial Pacific Ocean, which result in more rainfall over most parts of Myanmar, except for the south tip of country.

Table 4 Statistics of the leading SVD Pacific Ocean SST and rainfall modes

	Squared covariance	Temporal correlation	SST variance	Rainfall variance
Mode 1	48 %	0.74	33 %	16 %
Mode 2	31 %	0.80	14 %	20 %
Mode 3	8 %	0.79	13 %	6 %

SVD: Pacific SST vs. Myanmar rainfall

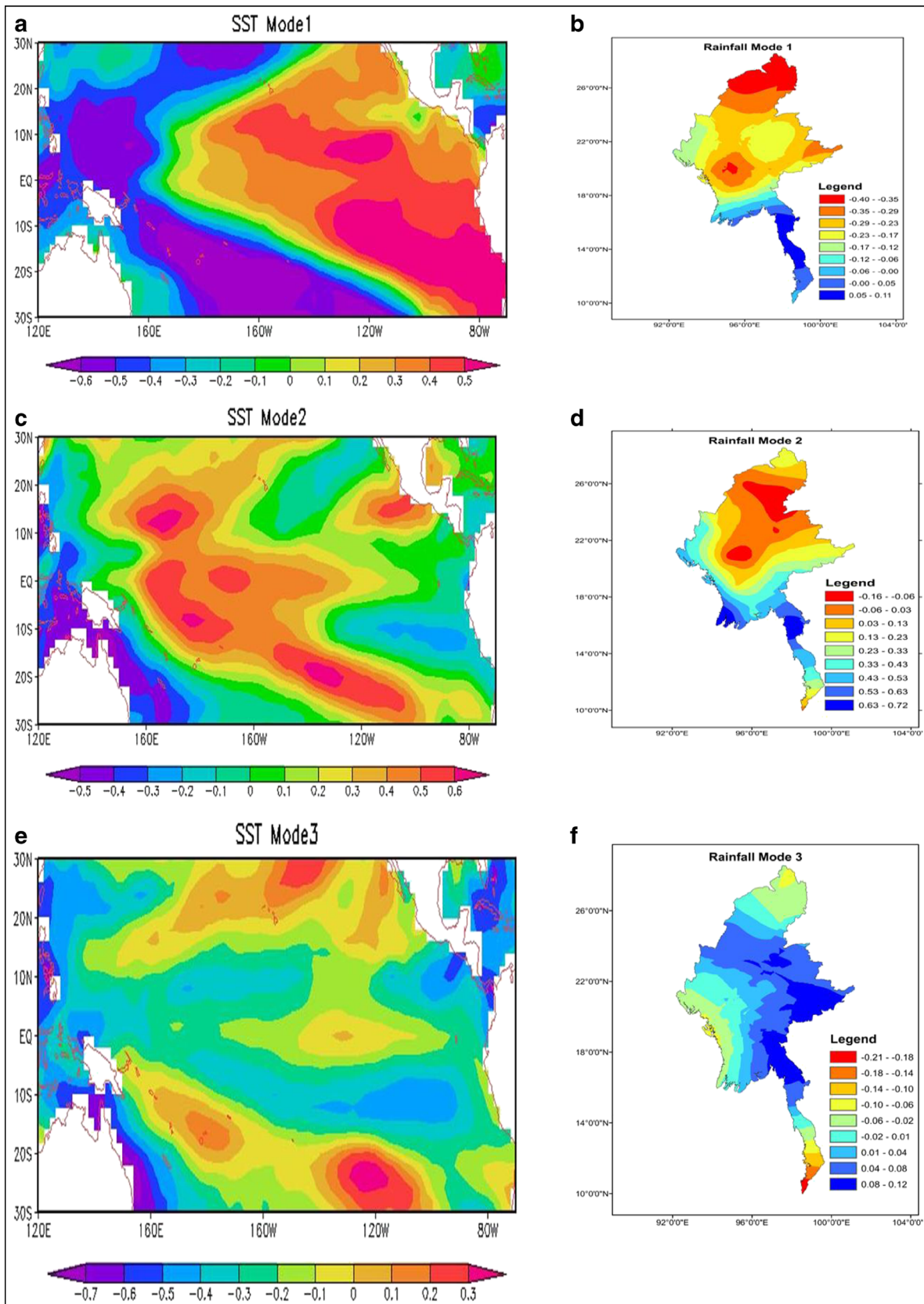
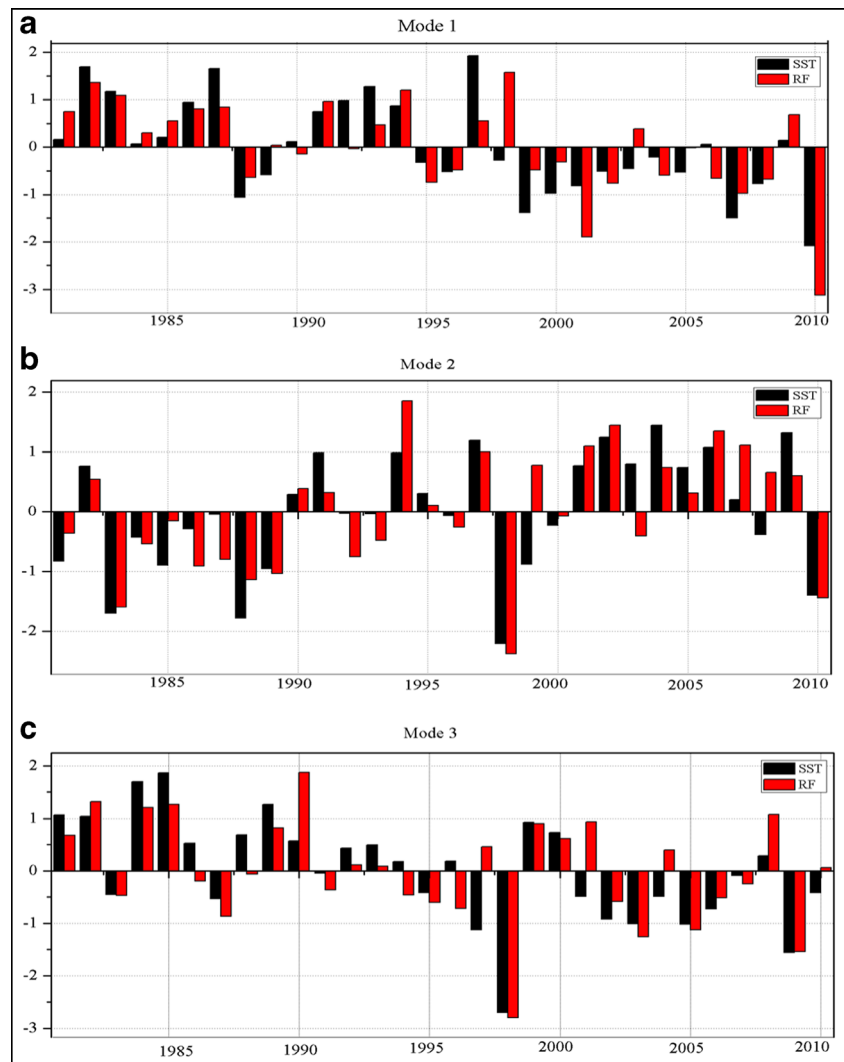


Fig. 17 Heterogeneous correlations of the first three SVD modes between Pacific SST (30° S–30° N) and Myanmar rainfall

Fig. 18 Normalized time series of the first three SVD modes for Pacific SST (*black bar*) and Myanmar Rainfall (*red bar*)



Acknowledgments This work was funded by the National Basic Research Program “973” of China (2012CB955200). The lead author is thankful to Chinese Scholarship Council and Nanjing University of Information Science and Technology for encouragement and for providing the necessary facilities to carry out this study. The authors also express their gratitude to ECMWF and NCEP/NCAR and Dr. Hrin Nei Thiam (Director General) of Department of Meteorology and Hydrology, Myanmar, for providing the data utilized in this study.

References

- Ahmed R, Karmakar S (1993) Arrival and withdrawal dates of the summer monsoon in Bangladesh. *Int J Climatol* 13:727–740
- Ali MM, Nagamani PV, Sharma N, Venu Gopal RT, Rajeevan M, Goni GJ, Bourassa Mark A (2015) Relationship between ocean mean temperatures and Indian summer monsoon rainfall. *AtmosSci Lett* 16:408–413
- Banacos PC, Schultz DM (2005) The use of moisture flux convergence in forecasting convective initiation: historical and operational perspectives. *Weather Forecast* 20:351–366
- Barry RG, Chorley RJ (2003) *Atmosphere, weather and climate*, 8th edn, 462 pp
- Bhowmik RSK, Durai VR (2008) Multi-model ensemble forecasting of rainfall over Indian monsoon region. *Atmosfera* 21:225–239
- Bretherton CS, Smith C, Wallace JM (1992) An intercomparison of methods for finding coupled patterns in climate data. *J Clim* 5:541–560
- Caesar JA, Alexander L, Vose R (2006) Large-scale changes in observed daily maximum and minimum temperatures—creation and analysis of a new gridded dataset. *J Geophys Res* 111:D05101. doi:10.1029/2005JD006280
- Caesar JA, Alexander LV, Trewin B, Tsering K, Sorany L, Vuniyayawa V, Keosavang N, Shimana A, Htay MM, Karmacharya J, Jayasinghearachchi DA, Sakkamart J, Soares E, Hung LT, Thuong LT, Hue CT, Dung NTT, Hung PV, Cuong HD, Cuong NM, Sirabaha S (2010) Changes in temperature and precipitation extremes over the indo-Pacific region from 1971 to 2005. *Int J Climatol* 31:791–801. doi:10.1002/joc.2118
- Chen TC, Weng SP (1999b) Maintenance of austral summertime upper-tropospheric circulation over tropical America: the Bolivian high–Nordeste low system. *J AtmosSci* 56:2081–2100
- Chen TC, Yen MC (1994) Interannual variation of the Indian monsoon simulated by the NCAR Community climate model: effect of the tropical Pacific SST. *J Clim* 7:1403–1415

- Dee DP, Uppala SM, Simmons AJ, et al. (2011) The ERA-Interim reanalysis: configuration and performance of the data assimilation system. *Q J R Meteorol Soc* 137:553–597
- Ding YH (1992) Summer monsoon rainfalls in China. *J Meteorol Soc Jpn* 70:373–396
- Dube SK, Luther ME, O'Brien JJ (1990) Relationships between interannual variability in the Arabian Sea and Indian summer monsoon rainfall. *Meteorol Atmosph Phys* 44:153–165
- Eguchi T (1996) Regional classification of the western part of the Indochina peninsula based on annual variation in precipitation, Research Reports of Department of Humanities, Faculty of Humanities and Economics, Kochi University: Kochi Jpn 4:1–9
- Ge F, Zhi XF, Babar ZA, Tang WW, Chen P (2016) Interannual variability of the summer monsoon precipitation over Indochina peninsula in association with ENSO. *Theor Appl Climatol*. doi:10.1007/s00704-015-1729-y
- Gilman DL, Fuglister FJ, Mitchell JM Jr (1963) On the power spectrum of “red noise”. *J Atmos Sci* 20:182–184
- Htway O, Matsumoto J (2011) Climatological onset dates of summer monsoon over Myanmar. *Int J Climatol* 31:382–393
- Huke R (1965) Rainfall in Burma. Geographical Publications, Dartmouth
- Joseph PV (2014) Role of ocean in the variability of Indian summer monsoon rainfall. *Surv Geophys* 35:723–738
- Joseph PV, Gokulapalan B, Nair A, Wilson SS (2013) Variability of summer monsoon rainfall in India on inter-annual and decadal time scales. *Atmos and Ocea Sci Let* 6:398–403
- Joshi MK, Pandey AC (2011) Trend and spectral analysis of rainfall over India during 1901–2000. *J Geophys Res* 116:D06104. doi:10.1029/2010JD014966
- Joshi P, Simon B, Desai P (1990) Atmospheric thermal changes over the Indian region prior to the monsoon onset as observed by satellite sounding data. *Int J Climatol* 10:49–56
- Juneng L, Tangang FT (2006) The covariability between anomalous northeast monsoon rainfall in Malaysia and sea surface temperature in Indian-Pacific Sector: a singular value decomposition analysis approach. *J Phys Sci* 17:101–115
- Kabanda TA, Jury MR (1999) Inter-annual variability of short rains over northern Tanzania. *Clim Res* 13:231–241
- Karl TR, Nicholls N, Ghazi A (1999) CLIVAR/GCOS/WMO workshop on indices and indicators for climate extremes: workshop summary. *Clim Chang* 42:3–7. doi:10.1023/A:1005491526870
- Kendall MG (1975) Rank Correlation Methods, 4th edn. Charles Griffin, London
- Kim C-J, Qian WH, Kang H-S, Lee D-K (2010) Interdecadal variability of east Asian summer monsoon precipitation over 220 years (1777–1997). *Adv Atmos Sci* 27:253–264. doi:10.1007/s00376-009-8079-6
- Krishnamurti TN, Bhalme HN (1976) Oscillations of a Monsoon System. Part I Observational Aspects. *J Atmos* 33:1937–1954
- Kumar S, Hazra A, Goswami BN (2014) Role of interaction between dynamics, thermodynamics and cloud microphysics on summer monsoon precipitating clouds over the Myanmar coast and the western Ghats. *Clim Dyn* 43:911–924
- Lau KM, Kim KM, Yang S (2000) Dynamical and boundary forcing characteristics of regional components of the Asian summer monsoon. *J Clim* 13:2461–2482
- Li XZ, Zhou W (2016) Modulation of the interannual variation of the India-Burma trough on the winter moisture supply over Southwest China. *Clim Dyn* 46:147–158. doi:10.1007/s00382-015-2575-4
- Lwin T (2000) The prevailing synoptic situations in Myanmar. A report submitted at the Workshop Agricultural Meteorology. Department of Meteorology and Hydrology, Yangon, Myanmar
- Mann H (1945) Nonparametric test against trend. *Econometrica* 13:245–259
- Mao J, Wu G (2007) Interannual variability in the onset of the summer monsoon over the Eastern Bay of Bengal. *Theor Appl Climatol* 89:155–170
- Maung MK (1945) Forecasting the coastal rainfall of Burma. *Q J R Meteorol Soc*
- May W (2004) Simulation of the variability and extremes of daily rainfall during the Indian summer monsoon for present and future times in a global time-slice experiment. *Clim Dyn* 22:183–204. doi:10.1007/s00382-003-0373-x
- Moe N (2002) Monsoon in Myanmar. Sarpay Beikman Press, Yangon, Myanmar, pp. 1–153
- Nalley D, Adamowski J, Khalil B, Ozga-Zielinski B (2013) Trend detection in surface air temperature in Ontario and Quebec, Canada during 1967–2006 using the discrete wavelet transform. *Atmos Res* 132:375–398
- Ogwang BA, Chen H, Tan G, Ongoma V, Ntwali D (2015) Diagnosis of East African climate and the circulation mechanisms associated with extreme wet and dry events: a study based on RegCM4. *Arab J Geosci*. doi:10.1007/s12517-015-1949-6
- Omondi PA, Awange JL, Forootan E, Ogollo LA, Barakiza R, Girmaw GB, Fesseha I, Kululetera V, Kileme C, Mbatii MM, Kilavi M, King'uyu SM, Omeny PA, Njogu A, Badr EM, Musa TA, Muchiri P BD, Komutunga E (2013) Changes in temperature and precipitation extremes over the Greater Horn of Africa region from 1961 to 2010. *Int J Climatol* 34:1262–1277
- Ongoma V, Muthama JN, Gitau W (2013) Evaluation of Urbanization Influences on Urban Temperature of Kenyan Cities. *Global Meteorol* 2(1). doi:10.4081/gm.2013.e1
- Ozer P, Mahamoud A (2013) Recent Extreme Precipitation and Temperature Changes in Djibouti City (1966–2011). *J Climatol*. doi:10.1155/2013/928501
- Pai DS, Nair RM (2009) Summer monsoon onset over Kerala: new definition and prediction. *Earth Syst Sci* 118:123–135
- Pant G, Kumar K (1997) Climate of South Asia. John Wiley and Sons, New York, USA
- Parthasarathy B, Munot AA, Kothawale DR (1994) All-India monthly and seasonal rainfall series: 1871–1993. *Theor Appl Climatol* 49:217–224
- PROMISE (2003) A project of European union. <http://ugamp.nerc.ac.uk/promise/brochure/brochure.pdf> (Accessed on 4/10/2014)
- Qian W, Lee DK (2000) Seasonal march of Asian summer monsoon. *Inter J Climatol* 20:1371–1386
- Rao YP (1976) Southwest monsoon. *Meteorol Monograph* (Synop Meteorol) India Meteorological Department, New Delhi, p. pp 366
- Sein ZMM, Ogwang BA, Ongoma V, Ogou FK, Batebana K (2015) Inter-annual variability of summer monsoon rainfall over Myanmar in relation to IOD and ENSO. *J Envir Agri Sci* 4:28–36
- Sen Roy N, Kaur S (2000) Climatology of monsoon rains of Myanmar (Burma). *Int J Climatol* 20:913–928
- Sen Roy S, Sen Roy N (2011) Influence of Pacific decadal oscillation and El Niño southern oscillation on the summer monsoon precipitation in Myanmar. *Int J Climatol* 31:14–21
- Smith TM, Reynolds RW, Peterson TC, Lawrimore J (2008) Improvements to NOAA's historical merged land-ocean surface temperature analysis (1880–2006). *J Clim* 21:2283–2296
- Sneyres R (1990) Technical note no. 143 on the statistical Analysis of Time Series of Observation. World Meteorological Organization, Geneva, Switzerland
- Tan GR, Ren HL, Chen H (2014) Quantifying synoptic eddy feedback onto the low-frequency flow associated with anomalous temperature events in January over China. *Int J Climatol*. doi:10.1002/joc.4135
- Tangang F (1999) Empirical orthogonal function analysis of precipitation anomaly in Malaysia. *Malay J Anal Sci* 5:155–165
- Waliser DE, Stern W, Schubert S, Lau KM (2003) Dynamic predictability of intraseasonal variability associated with the Asian summer monsoon. *Q J R Meteorol Soc* 129:2897–2925

- Wallace JM, Smith C, Bretherton CS (1992) Singular value decomposition of wintertime sea surface temperature and 500-mb height anomalies. *J Clim* 5:561–576
- Walsh JE, Mostek A (1980) A quantitative analysis of meteorological anomaly patterns over the United States, 1900–1977. *Mon Wea Rev* 108:615–630
- Wang B, Lin H (2002) Rainy Season of the Asian – Pacific Summer Monsoon. *J Clim* 15:386–398
- Yang H, Zhi XF, Gao J, Liu Y (2011) Variation of East Asian summer monsoon and its relationship with precipitation of China in recent 111 years. *AgricSciTechnol* 12:1711–1716
- Yoshino MM (1965) Four Stages of the Rainy Season in Early Summer over East Asia (Part II). *J Meteorol Soc Jpn* 43: 231–245
- Zhang L, Fraedrich K, Zhu X, Sielmann F, Zhi XF (2015) Interannual variability of winter precipitation in southeast China. *Theor Appl Clim* 119:229–238. doi:10.1007/s00704-014-1111-5
- Zhi XF (1997) Quasi-biennial oscillation in precipitation and its possible application to long-term prediction of floods and droughts over eastern China. *Ann Meteor* 35:250–252
- Zhi XF, Zhang L, Pan JL (2010) An analysis of the winter extreme precipitation events on the background of climate warming in southern China. *J Trop Meteorol* 16:325–332
- Zhu QG, Zhi XF (1991) Quasi-biennial oscillation in rainfall over China. *Acta Meteorol Sin* 5(4):426–434
- Zveryaev II, Aleksandrova MP (2004) Differences in rainfall variability in the South and Southeast Asian summer monsoons. *Int J Clim* 24: 1091–1107